



A comparative study of the performance of *E. coli* and *K. phaffii* for expressing α -cobratoxin

Damsbo, Anna; Rimbault, Charlotte; Burlet, Nick J.; Vlamynck, Anneline; Bisbo, Ida; Belfakir, Selma B.; Laustsen, Andreas H.; Rivera-de-Torre, Esperanza

Published in:
Toxicon

Link to article, DOI:
[10.1016/j.toxicon.2024.107613](https://doi.org/10.1016/j.toxicon.2024.107613)

Publication date:
2024

Document Version
Publisher's PDF, also known as Version of record

[Link back to DTU Orbit](#)

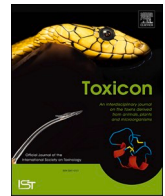
Citation (APA):
Damsbo, A., Rimbault, C., Burlet, N. J., Vlamynck, A., Bisbo, I., Belfakir, S. B., Laustsen, A. H., & Rivera-de-Torre, E. (2024). A comparative study of the performance of *E. coli* and *K. phaffii* for expressing α -cobratoxin. *Toxicon*, 239, Article 107613. <https://doi.org/10.1016/j.toxicon.2024.107613>

General rights

Copyright and moral rights for the publications made accessible in the public portal are retained by the authors and/or other copyright owners and it is a condition of accessing publications that users recognise and abide by the legal requirements associated with these rights.

- Users may download and print one copy of any publication from the public portal for the purpose of private study or research.
- You may not further distribute the material or use it for any profit-making activity or commercial gain
- You may freely distribute the URL identifying the publication in the public portal

If you believe that this document breaches copyright please contact us providing details, and we will remove access to the work immediately and investigate your claim.



A comparative study of the performance of *E. coli* and *K. phaffii* for expressing α -cobratoxin

Anna Damsbo^a, Charlotte Rimbault^a, Nick J. Burlet^a, Anneline Vlamynck^a, Ida Bisbo^a, Selma B. Belfakir^{a,b}, Andreas H. Laustsen^{a,*}, Esperanza Rivera-de-Torre^{a,*}

^a Department of Biotechnology and Biomedicine, Technical University of Denmark, DK-2800 Kongens Lyngby, Denmark

^b VenomAid Diagnostics ApS, DK-2800 Kongens Lyngby, Denmark

ARTICLE INFO

Handling Editor: Dr. Ray Norton

Keywords:

α -cobratoxin
Recombinant toxin expression
Snake venom
Yeast expression
Bacterial expression

ABSTRACT

Three-finger toxins (3FTxs) have traditionally been obtained via venom fractionation of whole venoms from snakes. This method often yields functional toxins, but it can be difficult to obtain pure isoforms, as it is challenging to separate the many different toxins with similar physicochemical properties that generally exist in many venoms. This issue can be circumvented via the use of recombinant expression. However, achieving the correct disulfide bond formation in recombinant toxins is challenging and requires extensive optimization of expression and purification methods to enhance stability and functionality. In this study, we investigated the expression of α -cobratoxin, a well-characterized 3FTx from the monocled cobra (*Naja kaouthia*), in three different expression systems, namely *Escherichia coli* BL21 (DE3) cells with the csCyDisCo plasmid, *Escherichia coli* SHuffle cells, and *Komagataella phaffii* (formerly known as *Pichia pastoris*). While none of the tested systems yielded α -cobratoxin identical to the variant isolated from whole venom, the His₆-tagged α -cobratoxin expressed in *K. phaffii* exhibited a comparable secondary structure according to circular dichroism spectra and similar binding properties to the $\alpha 7$ subunit of the nicotinic acetylcholine receptor. The findings presented here illustrate the advantages and limitations of the different expression systems and can help guide researchers who wish to express 3FTxs.

1. Introduction

Three-finger toxins (3FTxs) are a highly diverse group of toxins primarily present in the venom of snakes belonging to the *Elapidae* and *Colubridae* families (Tasoulis and Isbister, 2017). These toxins are characterized by a unique three-fingered fold, consisting of three loops or fingers protruding from a central β -sheet core, held together by four conserved disulfide bonds (Kini and Doley, 2010). While 3FTxs are typically known for their neurotoxicity and paralysis-inducing effects, this family of toxins has evolved to encompass a wide range of functions, including cytotoxic, anticoagulant, and cardiotoxic effects (Utkin, 2019).

The α -neurotoxins are a functional subgroup in the 3FTx family. They target postsynaptic nicotinic acetylcholine receptors (nAChRs), preventing acetylcholine from binding and activating these receptors. In

turn, this may ultimately cause flaccid paralysis and possibly death by asphyxiation in victims envenomed with these toxins (Barber et al., 2013; Nirthanen, 2020; Nirthanen and Gwee, 2004; Tsetlin et al., 2021). One well-studied member of this subgroup is α -cobratoxin, which is the medically most important toxin in the venom of the monocled cobra (*Naja kaouthia*) (Bourne et al., 2005; Laustsen et al., 2015; Osipov et al., 2012) and a widely utilized toxin in toxinology and antivenom research (Ledsgaard et al., 2023; Wade et al., 2022). α -cobratoxin is currently obtained through a labor-intensive process that involves capturing or breeding *N. kaouthia* snakes, followed by the potentially hazardous task of venom extraction (León et al., 2018; Sánchez et al., 2006). The purified toxin is then obtained using high-performance liquid chromatography (HPLC). This method presents significant challenges, including the dangers associated with snake handling and the potentially inconsistent quality of the purified toxin in different batches, as venom varies

Abbreviations: 3FTx, Three-finger toxin; nAChR, nicotinic acetylcholine receptor; PDI, Protein disulfide isomerase; SUMO, Small ubiquitin-like modifier; Ulp1, Ubiquitin-like-specific protease 1; CD, Circular dichroism; DELFIA, Dissociation-enhanced lanthanide fluorescence immunoassay.

* Corresponding author.

** Corresponding author.

E-mail addresses: ahola@bio.dtu.dk (A.H. Laustsen), erdto@dtu.dk (E. Rivera-de-Torre).

<https://doi.org/10.1016/j.toxicon.2024.107613>

Received 15 August 2023; Received in revised form 4 January 2024; Accepted 10 January 2024

Available online 11 January 2024

0041-0101/© 2024 The Authors. Published by Elsevier Ltd. This is an open access article under the CC BY license (<http://creativecommons.org/licenses/by/4.0/>).

with age, sex, diet, and environmental factors (Cipriani et al., 2017; Laustsen, 2019). To address these drawbacks, recombinant expression may be an alternative solution for obtaining a steady supply of toxins without the need to catch or keep snakes and extract their venom (de la Rosa et al., 2018; Liu et al., 2021; Lyukmanova et al., 2010; Makarova et al., 2018).

To express a correctly folded, functional recombinant toxin, it is necessary to find a recombinant expression system that can accommodate all the necessary features of the native toxin, including correct disulfide bond formation, and other post-translational modifications (Rivera-de-Torre et al., 2022). Common expression hosts, such as *Escherichia coli* and the yeast *Komagataella phaffii* (formerly known as *Pichia pastoris*), have their own advantages and disadvantages, making it relevant to compare their performance in expressing recombinant toxins (Rivera-de-Torre et al., 2022). *E. coli* is a widely used expression system due to the fast growth rate of this bacterium, the low cost of its media and other materials needed for its growth, and the ease of genetically manipulating this expression host. In this study, two different *E. coli*-based systems were used for the expression of α -cobratoxin, namely BL21 (DE3) cells with the csCyDisCo plasmid and SHuffle cells (Berkmen, 2012). SHuffle cells are designed to promote the formation of disulfide bonds, which are critical for proper folding and activity of 3FTxs, such as α -cobratoxin, while the csCyDisCo plasmid utilizes a co-expression of a sulfhydryl oxidase and two protein disulfide isomerases (PDIs) to improve the formation of disulfide bonds as well as the solubility of recombinant proteins (Bertelsen et al., 2021; Nielsen et al., 2019). In addition to the *E. coli*-based systems, the yeast, *K. phaffii* is a popular choice for protein expression due to its ability to secrete recombinant proteins, resulting in easier downstream processing. Furthermore, *K. phaffii* can perform post-translational modifications similar to those in higher organisms, including correct folding and disulfide bond formation (Karbalaei et al., 2020).

Here, we compare the expression of α -cobratoxin in *E. coli*, using both BL21 (DE3) cells with the csCyDisCo plasmid and Shuffle cells, and *K. phaffii*, with a focus on yield, purity, and functional activity of the recombinant toxin. By exploring the utility of each of these expression systems, we aim to facilitate the production of recombinant α -cobratoxin and other 3FTxs for research within toxinology, benefiting antivenom development and potentially unlocking the investigation of therapeutic applications for proteins based on this toxin scaffold (Rivera-de-Torre et al., 2022).

2. Material and methods

2.1. Plasmid construction

Recombinant α -cobratoxin was produced in *E. coli* using the plasmid pET39-His₆-SUMO- α -cobratoxin as previously described (Rimbault et al., 2023). Briefly, the gene encoding α -cobratoxin (Uniprot: P01391) was codon optimized for expression in bacteria and inserted into the pET39 vector with an N-terminal small ubiquitin-like modifier (SUMO) solubility tag. Other plasmids were created with a His₆-tag using the NEBuilder HiFi DNA Assembly Cloning Kit (New England Biolabs) following the manufacturer's instructions. The design of all primers for plasmid construction was performed using the NEBuilder Assembly Tool (New England Biolabs).

For expression in *K. phaffii*, the gene encoding His₆- α -cobratoxin was codon-optimized for expression in yeast and inserted into a pPICZ α A vector (Invitrogen) using the NEBuilder HiFi DNA Assembly Cloning Kit (New England Biolabs).

The coding sequences were cloned in phase with the α -mating factor of *S. cerevisiae* for secretion of the recombinant protein to the culture media and contained a His₆-tag on the N-terminal to streamline the purification. The resulting plasmids were verified by DNA sequencing to confirm the correct insertion of the α -cobratoxin gene and the respective tags (Eurofins Genomics) (Rimbault et al., 2023).

2.2. Expression of α -cobratoxin in *E. coli*

Two variations of α -cobratoxin constructs in the pET39 vector, namely His₆-SUMO- α -cobratoxin and His₆- α -cobratoxin, were transformed into chemically competent *E. coli* SHuffle cells (New England Biolabs). Similarly, BL21 (DE3) cells (Invitrogen) were transformed with the α -cobratoxins along with the csCyDisCo plasmid. The transformed SHuffle cells were plated on kanamycin-containing 2xYT (1.6% tryptone, 1% yeast extract, 0.5% NaCl) agar plates, while the BL21 (DE3) cells were plated on 2xYT agar plates supplemented with both kanamycin (50 μ g/mL) and chloramphenicol (20 μ g/mL). The plates for *E. coli* SHuffle cells were incubated at 30 °C according to the manufacturer's protocol, while the plates for BL21 (DE3) cells were incubated at 37 °C. For the overnight preculture, a 50 mL volume of 2xYT medium supplemented with kanamycin (50 μ g/mL) was inoculated with the transformed *E. coli* SHuffle cells and grown at 30 °C with continuous shaking at 220 rpm. In the case of BL21 (DE3), the medium was additionally supplemented with chloramphenicol (20 μ g/mL) and grown at 37 °C. The following day, a 1 L volume of 2xYT medium (1.6% tryptone, 1% yeast extract, 0.5% NaCl, 2 % (w/v) dextrose, 50 μ g/mL Kanamycin) was inoculated with the overnight preculture at an initial optical density at 600 nm (OD₆₀₀) of 0.1 and grown at 30 °C or 37 °C with continuous shaking at 220 rpm. The culture was allowed to reach an OD₆₀₀ of 0.8, at which point it was induced with 1 mM isopropyl β -D-1-thiogalactopyranoside (IPTG). In the case of BL21 (DE3), the medium was supplemented with chloramphenicol (20 μ g/mL).

Subsequently, the temperature was lowered to 16 °C, and the toxins were expressed for approximately 20 h. The next day, the cells were harvested by centrifugation at 6000 \times g for 15 min at 4 °C, and the cell pellets were subsequently resuspended in 30 mL lysis buffer (50 mM Tris-HCl, pH 8.0, 300 mM NaCl, and 20 mM imidazole) supplemented with lysozyme (1 mg/mL) and benzonase (1 μ L/50 mL). The cells were lysed on ice by sonication using a Fisherbrand FB120 sonicator, operated in pulsed mode with 90 cycles of 2-s intervals at 40% amplitude of vibration, with a 2-s pause in between pulses to avoid overheating. The soluble fraction was separated from the insoluble debris by centrifugation at 15,000 \times g for 30 min at 4 °C. The resulting clarified supernatants were collected and stored at 4 °C for subsequent purification steps.

2.3. Expression of α -cobratoxin in *K. phaffii*

The generation of electrocompetent *K. phaffii* cells followed a previously described protocol (Tapia-Galisteo et al., 2022). Briefly, plasmid DNA (10 μ g) was linearized using SacI digestion and electroporated into the KM71H strain using the Bio-Rad Gene Pulser apparatus (Bio-Rad, Hercules, CA, USA). Cells containing the integrated sequences were selected on YPDS plates (20 g/L peptone, 10 g/L yeast Extract, 20% (w/v) dextrose, 182.2 g/L sorbitol, 20 g/L agar) supplemented with increasing concentrations of Zeocin (100, 500, or 1000 μ g/mL).

Each individual clone was separately inoculated into 50 mL BMGY medium (10 g/L yeast extract, 20 g/L peptone, 0.1 M potassium phosphate pH 6.0, 1.34% (w/v) yeast nitrogen base (YNB), 0.04 μ g/mL biotin, 1% (v/v) glycerol) and incubated overnight at 30 °C with shaking at 220 rpm to assess the expression levels of different clones. The overnight cultures were centrifuged at 4,000 \times g for 10 min, and the resulting cell pellets were resuspended in 5 mL BMMY medium (10 g/L yeast extract, 20 g/L peptone, 0.1 M potassium phosphate pH 6.0, 1.34% (w/v) YNB, 0.04 μ g/mL biotin, 0.5% (v/v) methanol). The cultures were further incubated at 25 °C for 4 days with continuous shaking. Methanol was added to the cultures every 24 h at a final concentration of 0.5% (v/v) to maintain protein expression. To evaluate protein expression, 1000 μ L samples were taken from the cultures every 24 h. The samples were centrifuged at 5,000 \times g for 1 min, and the supernatants were subjected to sodium dodecyl sulfate–polyacrylamide gel electrophoresis (SDS-PAGE), stained with colloidal Coomassie blue to assess expression levels. Based on the expression analysis, the clone with the highest expression

level was selected for large-scale expression.

For large-scale expression, the selected clone was inoculated into 5 mL YPD medium (20 g/L peptone, 10 g/L yeast extract, 20% (w/v) dextrose) and incubated overnight at 30 °C with shaking at 200 rpm. The following day, 2.5 mL of the saturated culture was transferred to 1 L of BMGY medium and grown for 24 h at 30 °C with shaking at 200 rpm. The culture was then centrifuged at 5,000×g for 10 min, and the cell pellet was resuspended in 100 mL of BMMY. Similar to the test expression, the cells were further cultured at 25 °C for 4 days with the addition of methanol to a final concentration of 0.5% (v/v) every 24 h. After 96 h, the cells were harvested by centrifugation at 17,000×g for 30 min at 4 °C, and the supernatant was collected. The supernatant was sterilized by filtration through a 0.2 µm membrane filter (Millipore). The filtered supernatant was then stored at 4 °C for subsequent purification steps.

2.4. Preparation of the SUMO protease Ulp1 protease

The Ubiquitin-like-specific protease 1 (Ulp1) was purchased from Sigma-Aldrich (SAE0067), and the lyophilized protease was reconstituted in 100 µL water supplemented with 1 mM DTT.

2.5. Purification of α -cobratoxin and protease cleavage

The cleared cell lysate from the *E. coli* and the filtered supernatant from the *K. phaffii* were subjected to His-purification using gravity flow purification. First, 5 mL of equilibrated HIS-Select® Nickel Affinity Gel resin (Millipore, Burlington, USA) was washed and equilibrated with wash buffer A (50 mM Tris-HCl, pH 8.0, 300 mM NaCl, and 20 mM imidazole), was mixed with the supernatant and incubated at 4 °C for 1 h with end-over-end rotation. The resin was subsequently transferred into chromatography columns, and the flow-through fractions were collected. The columns were washed with a wash buffer A until the A_{280} of the eluent was <0.05. Then, the toxins were eluted using 5 column volumes (CV) of elution buffer (50 mM Tris-HCl, pH 8.0, 300 mM NaCl, 400 mM imidazole). The fractions containing the eluted toxins were dialyzed twice against dialysis buffer (50 mM Tris-HCl, pH 8.0, 300 mM NaCl) at 4 °C and subsequently concentrated using Amicon® Ultra-15 Centrifugal Filters (Millipore, Burlington, USA).

The removal of His₆-SUMO tag from α -cobratoxin was carried out using Ulp1 protease. Ulp1 was added at a concentration of 10 U per mg of toxin. To create a reducing environment necessary for the protease activity, 0.05 mM of DTT was included in the reaction mixture. The reactions were incubated at 30 °C for 1 h followed by an overnight incubation at 4 °C.

Subsequently, the cleaved toxins were subjected to a second purification step using HIS-Select Nickel Affinity Gel resin. Prior to binding the toxin-protease reactions, 2 mL of the resin was washed and equilibrated with wash buffer B (50 mM Tris-HCl, pH 8.0, 150 mM NaCl). The resin was then mixed with the toxin-protease reactions and incubated for 16–18 h with end-to-end rotation at 4 °C. The flow-through, containing the cleaved toxin without any His-tags, was collected. The resin was further washed with 6 CV of wash buffer B. The removed tags and proteases were eluted using 4 CV of elution buffer. Finally, the purified toxins were stored at –20 °C for subsequent use.

2.6. SDS-PAGE and Western Blotting

Samples were prepared using loading buffer with or without 1 mM DTT and subsequently denatured at 95 °C for at least 20 min. Gel electrophoresis was conducted using SDS-PAGE, and the resulting gels were stained with Coomassie Blue dye followed by destaining.

Following SDS-PAGE, proteins were transferred to an Immobilon-P membrane (Millipore). Blocking was performed using a solution composed of 100 mM Tris-HCl, 150 mM NaCl, and 0.1% Tween 20 (TBST) supplemented with 5% (w/v) milk. Membranes were washed in

TBST for 10 min, repeated twice with fresh buffer. Detection of His₆-tagged proteins was achieved through incubation with Anti-His₆ antibody - HRP, diluted to 1:500 (ThermoFisher MA1-21315-HRP). Visualization was accomplished using Clarity ECL Western Blotting substrate and the Bio-Rad ChemiDoc system according to the manufacturer's instructions.

2.7. Preparation of native α -cobratoxin

Native α -cobratoxin from *N. kaouthia* purified to homogeneity by chromatographic methods was purchased from Latoxan SAS (Portes-lès-Valence, France). The toxin was shipped in lyophilized form and used as a comparative control for the recombinantly expressed α -cobratoxin. The native α -cobratoxin was reconstituted in 50 mM Tris-HCl, pH 8, 150 mM NaCl, and either used directly or biotinylated as described below.

2.8. Biotinylation of α -cobratoxin

The native α -cobratoxin, as well as the recombinantly expressed variants, were biotinylated according to the manufacturer's recommendation, using a 10:1 M ratio of biotinylation reagent (Innolink Biotin 354 S, Merck) to toxin. Briefly, the biotinylation reagent, dissolved in dimethyl sulfoxide (DMSO), was added to the recombinant toxins in a small volume (constituting <5% of the final mixture). After a 90-min incubation at 25 °C, the biotinylated toxins were separated from the unbound biotinylation reagent using Amicon® Ultra-4 Centrifugal Filter Units with a 3 kDa membrane and subjected to four washes using 4 mL PBS at 8 °C. Protein concentration was determined at 280 nm using a NanoDrop and adjusted based on the protein sequence's theoretical extinction coefficient calculated with ProtParam (Expasy) (Walker, 2005). The degree of biotinylation was assessed by the A_{280}/A_{354} absorbance ratio, indicating a biotin:toxin molar ratio ranging from 1:1 to 1.5:1 across all tested α -cobratoxin variants.

2.9. Circular dichroism (CD) spectroscopy

To compare the secondary structures of the recombinant α -cobratoxins with the native counterpart, CD spectroscopy was performed following a previously described protocol (Rimbault et al., 2023). In short, the toxins were dialyzed against a 10 mM potassium phosphate buffer (pH 7.0). Far-UV CD measurements were conducted using a JASCO J-1500 spectrophotometer (Easton, MD, USA) equipped with a 0.1 mm quartz cuvette. The spectrum was recorded by performing 10 measurements between 250 nm and 190 nm, with a bandwidth of 0.1 nm and intervals of 1 nm. The scan speed was set at 50 nm/s.

A control was included to compare the fully denatured native α -cobratoxin. This was achieved by denaturing the protein with 1 mM DTT and boiling it at 95 °C for 20 min.

The acquired spectra were processed and smoothed using SpectraManager software (JASCO). Graphs depicting the CD spectra were generated using GraphPad Prism 10.

2.10. In vitro binding of nAChR

A blocking dissociation-enhanced lanthanide fluorescence immunoassay (DELFI) was performed to assess the binding ability of the different purified α -cobratoxins to the human $\alpha 7$ -acetylcholine receptor chimera, following a previously described protocol (Ledsgaard et al., 2022). Briefly, Black MaxiSorp plates (Nunc A/S, Roskilde, Denmark) were coated with 4 µg/mL $\alpha 7$ -AChR in PBS (200 ng/well). The plates were blocked using PBS +1% BSA and washed thoroughly with PBS-T (PBS with 0.1% Tween-20) followed by PBS before the toxins were added in 3-fold dilutions ranging from 20 µg/mL to 0.34 ng/mL. The signals were generated with europium-labelled streptavidin at a concentration of 0.2 µg/mL and detected using a VICTOR Nivo Multimode Microplate reader. Measurements were performed in duplicates and the

experiment was performed twice to ensure reproducibility. The data was analyzed in Graphpad Prism 10 with a nonlinear fit using 'ECanything', a variable slope model, while constraining the F-value to 50.

3. Results

3.1. Expression and purification of recombinant α -cobratoxin

Recombinant α -cobratoxin was expressed using three different systems: 1) csCyDisCo in *E. coli* BL21 (DE3), 2) genetically modified *E. coli* SHuffle, and 3) the yeast *K. phaffii*. The protein sequence of α -cobratoxin

is represented in Fig. 1A. Plasmids were constructed and verified by Sanger sequencing to confirm the correct constructs (Fig. 1B). In addition to expressing His₆- α -cobratoxin, α -cobratoxin was expressed in *E. coli* fused with a SUMO tag to enhance protein solubility during expression. The cleared cell lysates obtained from the *E. coli* expressions and the filtered supernatant from the *K. phaffii* expression were subjected to purification using HIS-Select® Nickel Affinity Gel resin (Fig. 1C, D, and E). Those α -cobratoxin constructs harboring a solubility fusion protein were further processed by removing the solubility tag with Ulp1 protease (Fig. 1F) in the presence of 0.05 mM DTT. The presence of DTT is crucial for enabling protease activity, but it is

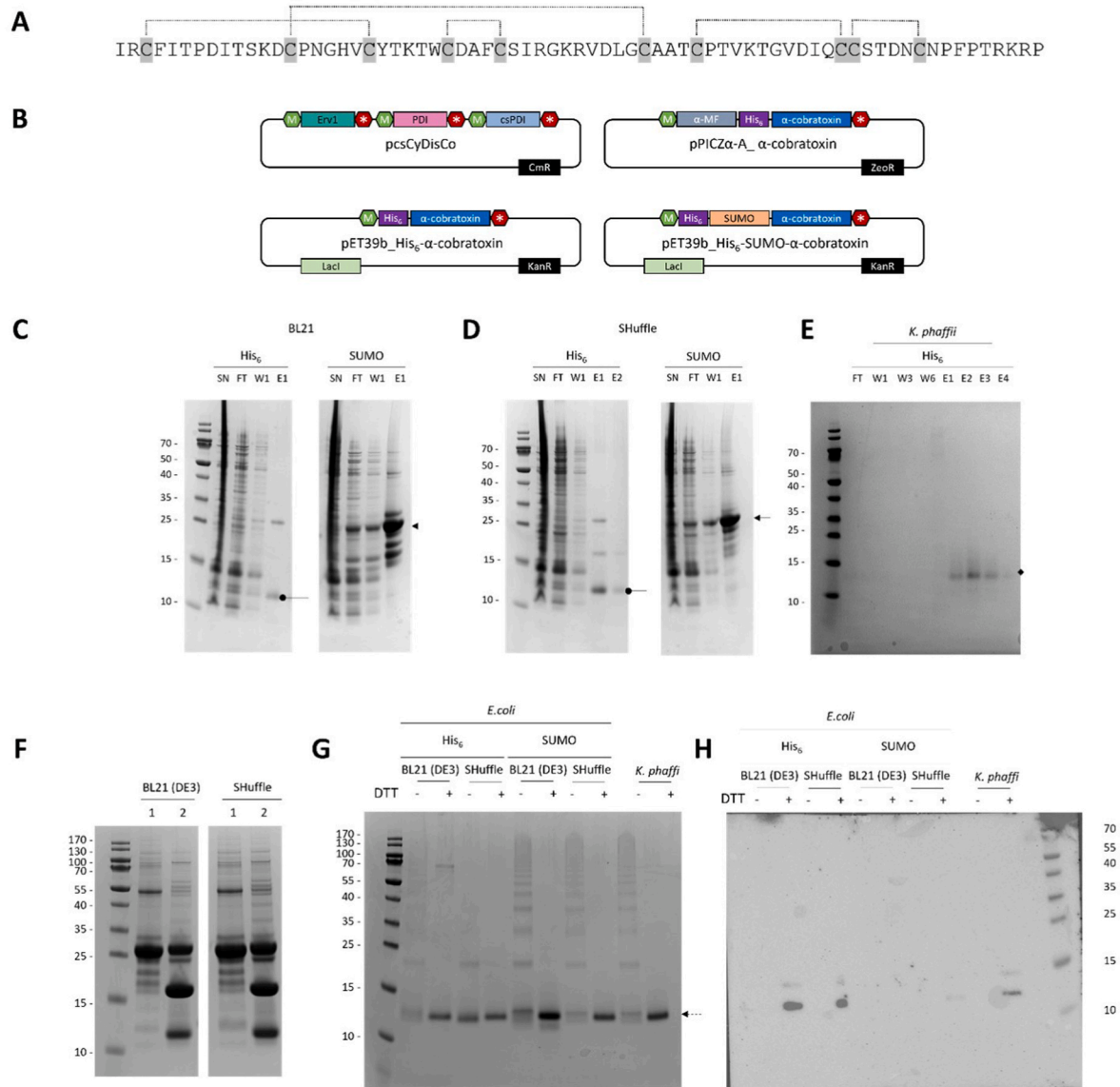


Fig. 1. Vector maps and gel pictures from the expression and purification of α -cobratoxin from *E. coli* and *K. phaffii*. **A)** Protein sequence of α -cobratoxin (accession number: P01391). The cysteines are highlighted in grey with the disulfide bond pattern indicated with dashed lines. **B)** The helper plasmid csCyDisCo containing the sulphhydryl oxidase Erv1 and the protein disulfide isomerases PDI and csPDI is shown, along with the three expression plasmids used for α -cobratoxin expression in different host systems. In *E. coli* expression, two constructs were used: His₆- α -cobratoxin and His₆-SUMO- α -cobratoxin. In *K. phaffii* expression, α -cobratoxin was fused with α -mating factor (α -MF) and a His₆-tag. **C)** The SDS-PAGE analysis of the first purification steps for *E. coli* BL21 (DE3) expression with the pcsCyDisCo co-expression system, **D)** *E. coli* SHuffle, and **E)** *K. phaffii*. The loaded samples include the supernatant after lysis (SN), flowthrough (FT), washes (WⁿXⁿ), and elution fractions (EⁿXⁿ). The migration of His₆- α -cobratoxin is indicated by a circle, and His₆-SUMO- α -cobratoxin by an arrowhead. **F)** The SDS-PAGE analysis demonstrates the protease cleavage of toxins containing a His₆-SUMO tag using Ulp1. The gel shows the samples before protease addition (1) and after overnight cleavage (2). **G)** SDS-PAGE analysis of the purified protein with 50 mM DTT or without DTT. Note that the tag-names are kept to make it easier to differentiate between the different toxin constructs, even though the tags are now removed. The observed migration shift after the addition of DTT suggests that disulfide bonds are present in the purified protein. The dashed arrow indicates the migration of α -cobratoxin. **H)** Western blot analysis under the same conditions assayed in the SDS-PAGE. The detection was performed with an anti-His₆-HRP antibody. Therefore, only the His₆- α -cobratoxin was detected.

essential to keep it as low as possible to minimize the reduction of disulfide bonds in the toxins. Subsequent experiments were conducted using the toxins after the removal of the tags. However, for clarity and to distinguish between the different constructs, the toxins are still referred to by their respective tag names. The molecular weights of the α -cobratoxin constructs are summarized in Table 1..

Subsequently, the purified toxin exhibited an electrophoretic mobility shift in the presence or absence of DTT, indicating disulfide bonds formed during the expression (Fig. 1G). Mobility shifts were also observed in the formerly SUMO-tagged α -cobratoxin, indicating that the disulfides remained intact after the proteolytic treatment. The mobility shift is notably different for the constructs assayed. The difference might be attributed to the heterogeneity in the disulfide-bond network which can alter electrophoretic migration due to the three-dimensional structure adopted the protein.

To authenticate the expressed toxins, a Western blot was carried out, analyzing the presence of the His₆-tag on the recombinant proteins (Fig. 1H). Bands corresponding to the expected mobility for His₆- α -cobratoxin were evident in wells containing recombinant proteins expressed in *E. coli* strains BL21 (DE3) csCyDisCo and SHuffle, as well as in yeast *K. phaffii*. Conversely, samples treated with Ulp1 displayed no positive signal, as the His₆-tag was linked to the N-terminal of the SUMO tag. Importantly, protein detection occurred only when samples were treated with DTT, suggesting inadequate exposure of the His₆-tag in the three-dimensional structure. This finding likely influences purification efficiency and highlights the need for optimization.

Table 2 summarizes the yield obtained from the different expression systems and plasmids used in this study for the expression of α -cobratoxin. The use of the *E. coli* SHuffle system resulted in a higher yield compared to the csCyDisCo system in BL21 (DE3) cells. Despite the initial impression of superior performance by His₆-SUMO compared to His₆, a substantial portion of the yield was lost during the second purification. In this relation, it is crucial to highlight that the SUMO tag, weighing more than the toxin itself, contributes to over 50% loss in mg during tag removal. However, as illustrated in Fig. 1F, the tag removal was not entirely complete. Notably, α -cobratoxin expressed solely with a His₆-tag performed well in both *E. coli* systems, even without being coupled to a solubility tag, and the expression of His₆- α -cobratoxin in *K. phaffii* resulted in a better yield compared to His₆- α -cobratoxin expressed in *E. coli*.

3.2. Characterization of the secondary structure of recombinant α -cobratoxins

Assessment of the folding and secondary structure of the recombinant α -cobratoxin samples was performed using CD spectroscopy, comparing them with the structure of the native α -cobratoxin and a denatured α -cobratoxin treated with 1 mM DTT and boiled at 95 °C for 20 min (Fig. 2).

The Far-UV CD spectra revealed important insights into the secondary structure of the proteins. The native α -cobratoxin shows spectrum characterized by a minimal value around 210 nm compatible with a secondary structure rich in β -sheet structures, as expected by its 3D-structure. It is also described that native α -cobratoxin shows a positive ellipticity peak centered around 228 nm, which is pH sensitive and believed to involve residues His18 and Tyr21, as well as the disulfide bonds within the hydrophobic core (Hider et al., 1982). Both

Table 1
Theoretical molecular weight of the recombinant α -cobratoxin constructs.

α -cobratoxin construct	MW before protease cleavage (kDa)	MW after protease cleavage (kDa)
His ₆ - α -cobratoxin	8.8	–
His ₆ -SUMO- α -cobratoxin	20.4	8.0

Table 2
Comparison of α -cobratoxin yields (mg per 1 L culture) using different expression systems. The table presents the yield of α -cobratoxin obtained from the use of different expression systems. The compared expression systems include *E. coli* SHuffle cells, *E. coli* BL21 (DE3) with the csCyDisCo plasmid, and *K. phaffii*. The yield is reported in milligrams per liter of culture volume.

Expression system	α -cobratoxin construct	Yield (mg per 1 L culture)	
		After the first purification	After protease cleavage
<i>E. coli</i> BL21(DE3) with csCyDisCo	His ₆ - α -cobratoxin	1.0	–
	His ₆ -SUMO- α -cobratoxin	7.2	0.6
<i>E. coli</i> SHuffle	His ₆ - α -cobratoxin	1.5	–
	His ₆ -SUMO- α -cobratoxin	10.0	0.8
<i>K. phaffii</i>	His ₆ - α -cobratoxin	3.0	–

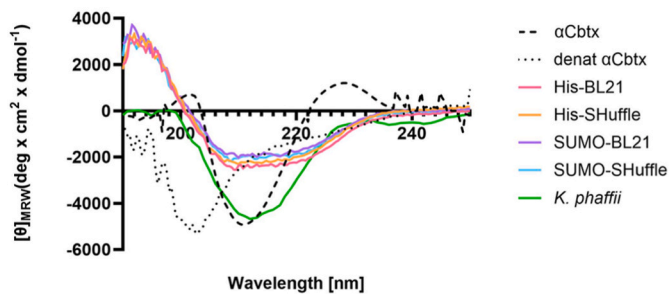


Fig. 2. CD spectra of the different α -cobratoxin constructs. The CD spectra of the various α -cobratoxin constructs were analyzed and compared to the native α -cobratoxin (α Cbtx). It is important to note that despite the tag being used as an identifier, the CD analysis was performed after tag removal by protease cleavage with the samples displayed in Fig. 1G.

characteristic points disappear when the toxin is completely denatured due to the action of reducing agents combined with heat, transforming the spectrum into one with a relative minimum ellipticity value at 205 nm compatible with a disordered structure.

Fig. 1G indicates the presence of disulfide bonds in the recombinant toxins produced in bacteria. However, the CD spectra for these constructs differ from the spectrum for the native α -cobratoxin. These differences may suggest that even though the recombinant α -cobratoxins produced in bacteria are forming disulfide bonds according to the electrophoretic mobility shift in the presence and absence of DTT, an unknown proportion of the total protein might not have the correct disulfide pattern, affecting the secondary structure of the proteins. Nevertheless, further experiments are needed to draw definitive conclusions in this regard.

The His₆- α -cobratoxin produced and expressed in *K. phaffii* showed a minimal ellipticity value at 212 nm and an intensity compatible with a structure rich in β -sheets comparable to the native α -cobratoxin. However, the characteristic maximum value registered around 228 nm for the native α -cobratoxin was not reproduced in the recombinant variant, probably due to slight modifications in the environment of the involved residues (His18 and Tyr21) or even the disposition of the disulfide bonds within the hydrophobic core of the toxin.

3.3. Assessment of the activity of the toxins through binding to an α 7-acetylcholine receptor chimera

The binding capacity of the recombinant α -cobratoxins to the human α 7-acetylcholine receptor chimera was evaluated using DELFIA binding assays. The purpose of this assessment was to determine if the recombinant toxins retained the ability to recognize and bind to the receptor subunit. Binding experiments were conducted using the α -cobratoxin

variants obtained from the different expression systems to compare their binding profiles (Fig. 3).

All recombinantly expressed α -cobratoxins demonstrated the ability to bind the $\alpha 7$ receptor in a manner similar to the native α -cobratoxin control. This indicates that all the expressed toxins, regardless of the conformational variability within the secondary structure level, maintained their recognition and interaction capabilities with the receptor.

The affinity of the His₆- and SUMO- α -cobratoxins respectively showed an average 2.6 and 4.1-fold decrease compared to native α -cobratoxin,. Even though the CD spectrum of the *K. phaffii* His₆- α -cobratoxin variant was more similar to native α -cobratoxin than the BL21 (DE3) and SHuffle His₆- α -cobratoxin variants, its binding ability to the receptor did not better resemble that of native α -cobratoxin. This suggests that although the conformations of the His₆- α -cobratoxins may be different, they do not significantly impair the binding capability of the toxin.

Taken together, these findings highlight that even though all the assayed systems yield functional toxins, the *K. phaffii*-expressed His₆- α -cobratoxin retained both its conformation and showed similar binding as the α -cobratoxin purified from the natural source. On the other hand, the recombinant α -cobratoxin variants produced in bacteria that have undergone a proteolytic cleavage from the His₆-SUMO tag exhibited a decreased EC₅₀ compared to the natural α -cobratoxin. These results thus provide insights into the functional integrity of the studied recombinant toxins and their suitability for further investigations and potential applications within toxinology and antivenom research.

4. Discussion

In this study, the expression of α -cobratoxin, a representative member of the 3FTx family, was achieved using three different systems: *E. coli* SHuffle cells, *E. coli* BL21 (DE3) with csCyDisCo, and *K. phaffii*. Each of these systems offers distinct advantages and limitations, making the choice of expression system dependent on the specific requirements of the protein.

In terms of post-translational modifications, disulfide bond formation is a critical aspect for the proper folding and function of 3FTxs, such as α -cobratoxin. However, despite the successful expression in all three systems, none of them yielded α -cobratoxin that was identical to the native variant. Nevertheless, the comparison of the different expression systems yielded valuable insights. In *E. coli* SHuffle cells, the use of the SUMO tag resulted in the highest titer, but inadequate cleavage during purification led to a lower final yield. Moreover, it was critical to optimize the concentration of DTT, necessary for protease cleavage using Ulp1, otherwise, the reducing agent reduces the disulfide bonds in the recombinant toxin. Even though the His₆-tagged variants lacking a

solubility partner showed lower yields in comparison with the His₆-SUMO versions, the purification process was faster, as they do not need to undergo a second purification step after cleavage. Thereby, the risk of reducing the disulfide bonds during the proteolysis step is evaded. This was confirmed by the different electrophoretic mobility assays performed in the presence or absence of DTT. Notably, the electrophoretic shift of the recombinant His₆- α -cobratoxin can be observed regardless of the bacterial system used for the expression (BL21 (DE3) or *E. coli* SHuffle) which means that the both strains are comparable regarding their capacity to form disulfide bonds.

The observed differences in CD spectra between the native α -cobratoxin and the recombinantly expressed toxins reveal that none of the recombinantly expressed α -cobratoxin variants have a structural conformation identical to the native protein purified from the natural source. The SDS-PAGE analysis with and without DTT suggests that disulfide bonds are formed in the recombinant α -cobratoxin variants. However, we lack information about the specific disulfide pairs formed in the recombinant systems. A single disulfide bond swap might lead to a slightly different fold compared to the native toxin, thereby affecting the overall secondary structure and causing the observed differences in the CD spectra. However, due to the limitations of the secondary purification process, drawing definitive conclusions about the folding proved challenging. Even though the proteins appear to be pure in the analytical SDS-PAGE (Fig. 1G), and the presence of unprocessed fusion proteins being negligible according to the Western blot analysis (Fig. 1H), the CD spectra may have also been affected by the presence of free fusion proteins and other impurities that were not entirely removed from the toxin samples. To establish a more conclusive assessment, further purification, and validation through e.g., size-exclusion chromatography or HPLC would be necessary.

The proteins expressed in *E. coli* without fusion proteins exhibit a folded structure with a similar fold to the one displayed by the processed His₆-SUMO variants. This structure is characterized by a β -sheet conformation consistent with the theoretical folding of α -cobratoxin. Similarly, the proteins expressed in *K. phaffii* also show a folded structure comparable to the native toxin purified from crude venom. When considering the CD spectrum of native α -cobratoxin, obtained through purification from the natural source using chromatographic methods, it is worth noting that the purified native α -cobratoxin exists as roughly 50% monomers and 50% dimers stabilized by intramolecular disulfide bonds, which may further complicate the interpretation of CD spectra and structural analyses of the recombinant toxins (Osipov et al., 2012; Modahl et al., 2016). This complexity makes it challenging to attribute the curvature of the CD spectrum solely to monomeric α -cobratoxin. Therefore, interpreting the native α -cobratoxin spectrum requires caution, considering the likelihood that it represents a mixture of at least

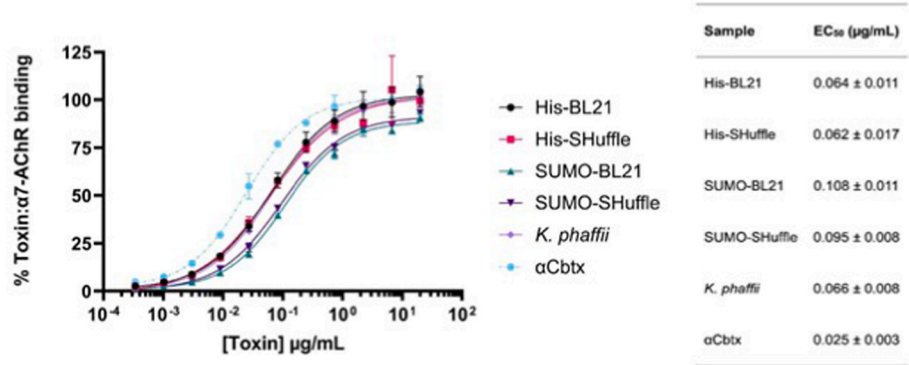


Fig. 3. Binding of recombinant α -cobratoxins to the $\alpha 7$ -subunit of nAChR. The α -cobratoxins expressed in the different expression systems were evaluated for their ability to bind the $\alpha 7$ -subunit of human nAChR. Even though the tag is written as the identifier, the DELFIA was conducted after tag removal by protease cleavage. Native α -cobratoxin (α Cbtx) was used as a positive control. The table presents the EC₅₀ values with corresponding standard deviations obtained from performing a nonlinear fit with a variable slope model.

two isoforms. Notably, the SDS-PAGE analysis of the recombinant proteins in the presence and the absence of DTT reveals that in the absence of DTT, the toxins also appear in multimeric forms, highlighted by the presence of bands with higher molecular weight, which disappear in the presence of the reducing agent. However, it is complex to estimate the proportion of multimeric structures present in the samples. It is also possible that the recombinantly expressed proteins contain multiple populations of α -cobratoxin variants with different disulfide bond patterns, causing the actual correctly folded α -cobratoxin to be only a fraction of the total polypeptides present. Therefore, further optimization of the expression systems and purification methods should be explored to enhance the formation of a correct disulfide bond pattern and ensure the structural stability (Glanville et al., 2022).

Interestingly, α -cobratoxin expressed in bacteria or yeast solely with a His₆-tag displayed similar binding behavior to the $\alpha 7$ subunit of the nAChR as the native α -cobratoxin, even though the EC₅₀ values were 2.6 times higher on average than the value registered for the toxin purified from the natural source. However, according to the CD spectra, the secondary structure of the His₆-tagged recombinant toxin differed from that of the native α -cobratoxin. This discrepancy might arise from the presence of the His₆-tag, indicating that while the His₆-tagged toxins maintain their binding capability, they may adopt a slightly altered conformation. Toxins obtained via proteolytic cleavage from the SUMO tag solubility partner exhibited an EC₅₀ value approximately four times greater than that of native α -cobratoxin. This reduction in binding affinity for the target receptor likely stems from an altered disulfide bond pattern. While maintaining the overall structure, this variant fails to replicate the three-dimensional fold necessary for optimal interaction with its target.

Recombinant toxins have been utilized to advance immunization strategies (Bermúdez-Méndez et al., 2018), offering a means to obtain pure and well-characterized toxins essential for antivenom development against snake venoms (de la Rosa et al., 2018, 2019). Furthermore, genetic engineering of snake toxins enables the exploration of new therapeutic possibilities, exemplified by engineered toxin variants like modified α -cobratoxin. Such approaches may thus help facilitate experimentation with toxin scaffolds to explore the potential design of non-toxic or less toxic versions with exploitable bioactive properties for therapeutic purposes (Fonar et al., 2021; Oliveira et al., 2022).

In contrast to previous studies on the expression of 3FTxs, this study highlights the challenges encountered in producing correctly folded α -cobratoxin. Glanville et al. utilized HEK cells to produce various 3FTxs and demonstrated their utility as antigens in phage display experiments (Glanville et al., 2022). Similarly, Liu et al. employed *E. coli* BL21 (DE3) and Rosetta (DE3) to express 3FTxs fused to DsbC and demonstrated that they could be used as immunogens to generate polyclonal sera that could neutralize whole venoms from three different cobras (Liu et al., 2021). While the correct folding of the toxin might be less crucial for immunizations, where the antigen undergoes processing by the immune system, there is no such processing involved in antibody phage display selection experiments. The successful selection of high-affinity antibodies depends almost entirely on molecular recognition, and, therefore, the correct folding of both toxin and antibody fragment is critical. Even though antibodies are known to also recognize linear epitopes, for *in vitro* display-based discovery approaches, structural integrity, correct folding, and post-translational modifications play an important role.

In conclusion, this study highlights the potential of recombinant toxin expression as a reliable and scalable source of protein-based toxins, thereby providing new opportunities to study venomous organisms and conduct research within toxinology and antivenom development. The choice of optimal expression system is crucial and should be done with the final application of the toxin variant to be expressed in mind. Further optimization of the protocols described here is needed to ensure that they deliver correctly folded toxins that retain proper recognition and binding to their target. Nevertheless, we hope that the methods and data presented can aid researchers who aim to express and

investigate α -cobratoxins, 3FTxs, and variants thereof.

Funding

This research was funded by the Villum Foundation (Grant No. 00025302), the European Research Council (ERC) under the European Union's Horizon 2020 research and innovation programme (Grant No. 850974), Innovation Fund Denmark (Grant No. 2052-00023B), and Wellcome Trust (Grant No. 221702/Z/20/Z). We also thank the following foundations for financial support: Danmark-Amerika Fondet, Otto Mønsted Fond, Augustinus Fonden, Knud Højgaards Fond, William Demant Fonden, and Torben og Alice Frimodts Fond.

Ethical statement

No experimentation on human or animal subjects was involved in this study.

CRediT authorship contribution statement

Anna Damsbo: Writing – review & editing, Writing – original draft, Visualization, Validation, Methodology, Investigation, Conceptualization. **Charlotte Rimbault:** Writing – review & editing, Supervision, Investigation, Conceptualization. **Nick J. Burlet:** Writing – review & editing, Visualization, Validation, Methodology, Investigation. **Anne-line Vlaminck:** Writing – review & editing, Investigation. **Ida Bisbo:** Writing – review & editing, Investigation. **Selma B. Belfakir:** Writing – review & editing, Writing – original draft, Visualization, Methodology, Investigation. **Andreas H. Laustsen:** Writing – review & editing, Writing – original draft, Visualization, Validation, Supervision, Resources, Project administration, Methodology, Investigation, Funding acquisition, Conceptualization. **Esperanza Rivera-de-Torre:** Writing – review & editing, Writing – original draft, Visualization, Validation, Supervision, Project administration, Methodology, Investigation, Conceptualization.

Declaration of competing interest

The authors declare that they have no known competing financial interests or personal relationships that could have appeared to influence the work reported in this paper.

Data availability

Data will be made available on request.

References

- Barber, C.M., Isbister, G.K., Hodgson, W.C., 2013. Alpha neurotoxins. *Toxicon* 66, 47–58. <https://doi.org/10.1016/j.toxicon.2013.01.019>.
- Berkmen, M., 2012. Production of disulfide-bonded proteins in *Escherichia coli*. *Protein Expr. Purif.* 82, 240–251. <https://doi.org/10.1016/j.pep.2011.10.009>.
- Bermúdez-Méndez, E., Fuglsang-Madsen, A., Føns, S., Lomonte, B., Gutiérrez, J.M., Laustsen, A.H., 2018. Innovative Immunization Strategies for Antivenom Development. *Toxins* 10, 452. <https://doi.org/10.3390/toxins10110452>.
- Bertelsen, A.B., Hackney, C.M., Bayer, C.N., Kjelgaard, L.D., Rennig, M., Christensen, B., Sørensen, E.S., Safavi-Hemami, H., Wulff, T., Ellgaard, L., Nørholm, M.H.H., 2021. DisCoTune: versatile auxiliary plasmids for the production of disulphide-containing proteins and peptides in the *E. coli* T7 system. *Microb. Biotechnol.* 14, 2566–2580. <https://doi.org/10.1111/1751-7915.13895>.
- Bourne, Y., Talley, T.T., Hansen, S.B., Taylor, P., Marchot, P., 2005. Crystal structure of a Cbtx-AChBP complex reveals essential interactions between snake alpha-neurotoxins and nicotinic receptors. *EMBO J.* 24, 1512–1522. <https://doi.org/10.1038/sj.emboj.7600620>.
- Cipriani, V., Debono, J., Goldenberg, J., Jackson, T.N.W., Arbuckle, K., Dobson, J., Koludarov, I., Li, B., Hay, C., Dunstan, N., Allen, L., Hendrikx, I., Kwok, H.F., Fry, B. G., 2017. Correlation between ontogenetic dietary shifts and venom variation in Australian brown snakes (*Pseudonaja*). *Comp. Biochem. Physiol. C Toxicol. Pharmacol.* 197, 53–60. <https://doi.org/10.1016/j.cbpc.2017.04.007>.
- de la Rosa, G., Corrales-García, L.L., Rodríguez-Ruiz, X., López-Vera, E., Corzo, G., 2018. Short-chain consensus alpha-neurotoxin: a synthetic 60-mer peptide with generic

- traits and enhanced immunogenic properties. *Amino Acids* 50, 885–895. <https://doi.org/10.1007/s00726-018-2556-0>.
- de la Rosa, G., Olvera, F., Archundia, I.G., Lomonte, B., Alagón, A., Corzo, G., 2019. Horse immunization with short-chain consensus α -neurotoxin generates antibodies against broad spectrum of elapid venomous species. *Nat. Commun.* 10, 3642. <https://doi.org/10.1038/s41467-019-11639-2>.
- Fonar, G., Polis, B., Sams, D.S., Levi, A., Malka, A., Bal, N., Maltsev, A., Elliott, E., Samson, A.O., 2021. Modified snake α -neurotoxin averts β -amyloid binding to $\alpha 7$ nicotinic acetylcholine receptor and reverses cognitive deficits in alzheimer's disease mice. *Mol. Neurobiol.* 58, 2322. <https://doi.org/10.1007/s12035-020-02270-0>.
- Glanville, J., Andrade, J.C., Bellin, M., Kim, S., Pletnev, S., Tsao, D., Verardi, R., Bedi, R., Friede, T., Liao, S., Newland, R., Bayless, N.L., Youssef, S., Tully, E., Zhang, B., Bylund, T., Kim, S., Liu, T., Kwong, P.D., 2022. Venom protection by antibody from a snakebite hyperimmune subject. <https://doi.org/10.1101/2022.09.26.507364>, 2022.09.26.507364.
- Hider, R.C., Drake, A.F., Inagaki, F., Williams, R.J.P., Endo, T., Miyazawa, T., 1982. Molecular conformation of α -cobratoxin as studied by nuclear magnetic resonance and circular dichroism. *J. Mol. Biol.* 158, 275–291. [https://doi.org/10.1016/0022-2836\(82\)90433-8](https://doi.org/10.1016/0022-2836(82)90433-8).
- Karbalaei, M., Rezaee, S.A., Farsiani, H., 2020. Pichia pastoris: a highly successful expression system for optimal synthesis of heterologous proteins. *J. Cell. Physiol.* 235, 5867–5881. <https://doi.org/10.1002/jcp.29583>.
- Laustsen, A., 2019. How can monoclonal antibodies be harnessed against neglected tropical diseases and other infectious diseases? *Expert Opin. Drug Discov.* 14, 1–10. <https://doi.org/10.1080/17460441.2019.1646723>.
- Laustsen, A., Gutiérrez, J., Lohse, B., Rasmussen, A., Fernandez Ulate, J., Milbo, C., Lomonte, B., 2015. Snake venomomics of monocled cobra (*Naja kaouthia*) and investigation of human IgG response against venom toxins. *Toxicon: Official Journal of the International Society on Toxinology.* 99 <https://doi.org/10.1016/j.toxicon.2015.03.001>.
- L. Ledsgaard, A.H. Laustsen, U. Pus, J. Wade, P. Villar, K. Boddum, P. Slavny, E.W. Masters, A.S. Arias, S. Oscos, D.T. Griffiths, A.M. Luther, M. Lindholm, R.A. Leah, M. S. Möller, H. Ali, J. McCafferty, B. Lomonte, J.M. Gutiérrez, A. Karatt-Vellatt, 2022. In vitro discovery of a human monoclonal antibody that neutralizes lethality of cobra snake venom. *mAbs.* 14. doi:10.1080/19420862.2022.2085536.
- Ledsgaard, L., Wade, J., Jenkins, T.P., Boddum, K., Oganessian, I., Harrison, J.A., Villar, P., Leah, R.A., Zenobi, R., Schoffelen, S., Voldborg, B., Ljungars, A., McCafferty, J., Lomonte, B., Gutiérrez, J.M., Laustsen, A.H., Karatt-Vellatt, A., 2023. Discovery and optimization of a broadly-neutralizing human monoclonal antibody against long-chain α -neurotoxins from snakes. *Nat. Commun.* 14, 682. <https://doi.org/10.1038/s41467-023-36393-4>.
- León, G., Vargas, M., Segura, A., Herrera, M., Villalta, M., Sánchez, A., Solano, G., Gómez, A., Sánchez, M., Estrada, R., Gutiérrez, J.M., 2018. Current technology for the industrial manufacture of snake antivenoms. *Toxicon* 151, 63–73. <https://doi.org/10.1016/j.toxicon.2018.06.084>.
- Liu, B.-S., Jiang, B.-R., Hu, K.-C., Liu, C.-H., Hsieh, W.-C., Lin, M.-H., Sung, W.-C., 2021. Development of a broad-spectrum antiserum against cobra venoms using recombinant three-finger toxins. *Toxins* 13, 556. <https://doi.org/10.3390/toxins13080556>.
- Lyukmanova, E.N., Shulepko, M.A., Shenkarev, Z.O., Dolgikh, D.A., Kirpichnikov, M.P., 2010. In vitro production of three-finger neurotoxins from snake venoms, a disulfide rich proteins. Problems and their solutions (Review). *Russ. J. Bioorg. Chem.* 36, 137–145. <https://doi.org/10.1134/S1068162010020019>.
- Makarova, YaV., Kryukova, E.V., Shelukhina, I.V., Lebedev, D.S., Andreeva, T.V., Ryazantsev, D.Yu., Balandin, S.V., Ovchinnikova, T.V., Tsetlin, V.I., Utkin, YuN., 2018. The first recombinant viper three-finger toxins: inhibition of muscle and neuronal nicotinic acetylcholine receptors. *Dokl. Biochem. Biophys.* 479, 127–130. <https://doi.org/10.1134/S1607672918020205>.
- Modahl, C.M., Mukherjee, A.K., Mackessy, S.P., 2016. An analysis of venom ontogeny and prey-specific toxicity in the Monocled Cobra (*Naja kaouthia*). *Toxicon* 119, 8–20. <https://doi.org/10.1016/j.toxicon.2016.04.049>.
- Nielsen, L.D., Foged, M.M., Albert, A., Bertelsen, A.B., Søltøft, C.L., Robinson, S.D., Petersen, S.V., Purcell, A.W., Olivera, B.M., Norton, R.S., Vasskog, T., Safavi-Hemami, H., Teilum, K., Ellgaard, L., 2019. The three-dimensional structure of an H-superfamily conotoxin reveals a granulin fold arising from a common ICK cysteine framework. *J. Biol. Chem.* 294, 8745–8759. <https://doi.org/10.1074/jbc.RA119.007491>.
- Nirthanan, S., 2020. Snake three-finger α -neurotoxins and nicotinic acetylcholine receptors: molecules, mechanisms and medicine. *Biochem. Pharmacol.* 181, 114168. <https://doi.org/10.1016/j.bcp.2020.114168>.
- Nirthanan, S., Gwee, M.C.E., 2004. Three-finger alpha-neurotoxins and the nicotinic acetylcholine receptor, forty years on. *J. Pharmacol. Sci.* 94, 1–17. <https://doi.org/10.1254/jphs.94.1>.
- Oliveira, A.L., Viegas, M.F., da Silva, S.L., Soares, A.M., Ramos, M.J., Fernandes, P.A., 2022. The chemistry of snake venom and its medicinal potential. *Nat. Rev. Chem.* 6, 451–469. <https://doi.org/10.1038/s41570-022-00393-7>.
- Osipov, A.V., Rucktooa, P., Kasheverov, I.E., Filkin, S.Y., Starkov, V.G., Andreeva, T.V., Sixma, T.K., Bertrand, D., Utkin, Y.N., Tsetlin, V.I., 2012. Dimeric α -cobratoxin X-ray structure: localization of intermolecular disulfides and possible mode of binding to nicotinic acetylcholine receptors. *J. Biol. Chem.* 287, 6725–6734. <https://doi.org/10.1074/jbc.M111.322313>.
- Rimbault, C., Knudsen, P.D., Damsbo, A., Boddum, K., Ali, H., Hackney, C.M., Ellgaard, L., Bohn, M.-F., Laustsen, A.H., 2023. A single-chain variable fragment selected against a conformational epitope of a recombinantly produced snake toxin using phage display. *N. Biotech.* 76, 23–32. <https://doi.org/10.1016/j.nbt.2023.04.002>.
- Rivera-de-Torre, E., Rimbault, C., Jenkins, T.P., Sørensen, C.V., Damsbo, A., Saez, N.J., Duhoo, Y., Hackney, C.M., Ellgaard, L., Laustsen, A.H., 2022. Strategies for heterologous expression, synthesis, and purification of animal venom toxins. *Front. Bioeng. Biotechnol.* 9 <https://doi.org/10.3389/fbioe.2021.811905>.
- Sánchez, E., Pérez, J., Powell, R., 2006. Farming for venom: survey of snake venom extraction facilities worldwide. *Appl. Herpetol.* 3, 1–10. <https://doi.org/10.1163/157075406775247067>.
- Tapia-Galisteo, A., Sánchez Rodríguez, Í., Aguilar-Sopeña, O., Harwood, S.L., Narbona, J., Ferreras Gutierrez, M., Navarro, R., Martín-García, L., Corbacho, C., Compte, M., Lacadena, J., Blanco, F.J., Chames, P., Roda-Navarro, P., Álvarez-Vallina, L., Sanz, L., 2022. Trispecific T-cell engagers for dual tumor-targeting of colorectal cancer. *Oncotarget* 11, 2034355. <https://doi.org/10.1080/2162402X.2022.2034355>.
- Tasoulis, T., Isbister, G.K., 2017. A review and database of snake venom proteomes. *Toxins* 9, 290. <https://doi.org/10.3390/toxins9090290>.
- Tsetlin, V.I., Kasheverov, I.E., Utkin, Y.N., 2021. Three-finger proteins from snakes and humans acting on nicotinic receptors: old and new. *J. Neurochem.* 158, 1223–1235. <https://doi.org/10.1111/jnc.15123>.
- Utkin, Y.N., 2019. Last decade update for three-finger toxins: newly emerging structures and biological activities. *World J. Biol. Chem.* 10, 17–27. <https://doi.org/10.4331/wjbc.v10.i1.17>.
- Wade, J., Rimbault, C., Ali, H., Ledsgaard, L., Rivera-de-Torre, E., Abou Hachem, M., Boddum, K., Mirza, N., Bohn, M.-F., Sakya, S.A., Ruso-Julve, F., Andersen, J.T., Laustsen, A.H., 2022. Generation of multivalent nanobody-based proteins with improved neutralization of long α -neurotoxins from elapid snakes. *Bioconjugate Chem.* 33, 1494–1504. <https://doi.org/10.1021/acs.bioconjchem.2c00220>.
- Walker, J.M. (Ed.), 2005. *The Proteomics Protocols Handbook*. Humana Press, Totowa, NJ. <https://doi.org/10.1385/1592598900>.